

On the Right Track? Designing Optimal Public Transit Contracts

Matías Navarro*
Cornell University

Job Market Paper | September 23, 2025

[Please click here for the latest version](#)

Abstract

Private transit provision under weak regulation creates two key inefficiencies: market power leading to underprovision, and uninternalized network effects where firms fail to consider how service on one route affects demand across the network. To address these market failures, governments increasingly use contracts with private operators featuring quality targets and route bundling. This paper studies how these contract instruments should be designed to maximize welfare. The key challenge is that underlying market failures push policy in opposite directions: increasing competition mitigates market power but can fragment service and weaken network coordination. I exploit unique quasi-experimental variation from Santiago, Chile's large-scale 2022 contract reform, which imposed stricter quality targets and rebundled routes among private operators. Using high-frequency GPS tracking data from 373 bus routes and an event-study difference-in-differences design, I find that stricter quality targets improve service regularity by 17.1% and increase ridership by 7.5%. I develop and estimate a structural model incorporating traveler demand and operator costs to study optimal contract design. Results show welfare losses from monopoly pricing outweigh network gains from single-operator coordination, with optimal market structure involving four to five competing firms. Route bundle composition plays a critical role in preserving network connectivity while balancing costs and network effect internalization.

Keywords: Public Transit. Private Provision. Contracts. Network Effects. JEL: D22, D62, L91, L92, R41, R42

*Dyson School of Applied Economics and Management, Cornell University (Email: min26@cornell.edu). I am grateful to my advisors Shanjun Li, Todd Gerarden, Andrew Waxman, and Stuart Rosenthal for invaluable advice and support, and to Seba Tamblay, Beia Spiller, and seminar participants at Cornell University, AERE Summer Conference, ITEA Annual Conference for helpful comments. I gratefully acknowledge support by the Interdisciplinary Transportation Doctoral Fellowship funded by the Alfred P. Sloan Foundation. All errors are mine.

1 Introduction

Governments delegate a large share of public service delivery to private firms, with public procurement accounting for 12% of global GDP (Bosio *et al.*, 2022). This is especially true in sectors such as energy distribution, broadband, and transportation, where service quality and access are critical. In the case of private provision of public transit, weak or absent regulation often leads to inefficiencies, including high prices, poor service quality, and gaps in network coverage (Conwell, 2023; Mbonu and Eaglin, 2024). Economic theory rationalizes these inefficiencies through two market failures: market power, which leads to markups and suboptimal service quality, and uninternalized network effects, where independent operators may fail to account for network complementarities.

In recent decades, many transit agencies have adopted contractual approaches to regulate service provision (see Figure C.1 for examples across cities). While these contracts vary across multiple design dimensions, two are particularly relevant as they directly target the market failures described above. The first is quality targets, which impose minimum service standards to curb underprovision, creating a trade-off between service quality and provision costs as firms face performance penalties when GPS monitoring reveals deviations. The second is route bundling, specifically, how many routes to group into each contract to balance competition and coordination. Smaller bundles foster price competition through more bidders but can fragment the network; larger bundles preserve coordination but may reduce competitive pressure. Despite their widespread use, we know little about how quality targets and route bundling interact through their respective trade-offs. This leaves unresolved how to design contracts that maximize welfare when market power and network effects pull in opposing directions.

In this paper, I study how quality targets and route bundling interact in addressing market power and network effects in public transit contracts.

I explore this question in the context of Santiago de Chile's public transit system, Transantiago, one of the first large-scale systems to adopt contracts for bus service provision. Transantiago incentivizes private provision of bus service through competitively awarded operating contracts to several private firms. Contracts compensate firms for service provision based on kilometers traveled and passengers transported, and specify obligations on service attributes such as frequency and regularity. Transantiago contracts pay transit firms about \$840 million dollars per year to operate more than 350 routes that serve, jointly with the subway network, approximately 3 million trips per day. These contracts typically last for five to seven years.

In 2022, Transantiago contracts underwent a major reform, providing a unique empirical setting to study how firms respond to changes in contract structure. The reform affected over 30 percent of the network, modifying both the stringency of quality targets

and the size and composition of route bundles. To study these contract redesigns, I combine a rich set of administrative data, including a household travel survey, smart card fare validations, and GPS records from all transit vehicles. These sources allow me to link travelers' mode and route choices to route-level service attributes—such as frequency and headway regularity—measured at fine spatial and temporal resolution. Moreover, the insights from this setting are broadly applicable: Santiago's contractual framework is representative of other large cities that rely on competitive tendering to regulate privately operated transit networks.

I analyze the market failures that arise in public transit provision using a conceptual framework adapted from Barwick *et al.* (2024), who study attribute-based subsidies in a standard price-attribute space. In my setting, a monopolist chooses both prices and service attributes—such as frequency and headway regularity—while a social planner chooses the same variables to maximize welfare. I extend the framework by allowing travelers' willingness to pay for service on one route to depend on service levels elsewhere in the network, introducing demand-side network effects. Both the monopolist and the social planner internalize these effects. However, the monopolist both underprovides service quality, ignoring the environmental externality of shifting travelers from cars to transit, and charges a markup due to market power. These two distortions motivate the contractual instruments I study: quality targets, which can restore efficient service levels if penalties reflect the externality but leave the markup distortion intact, and route bundling, which reduces markups by introducing competition but fragments the network, weakening coordination. This trade-off between competition and coordination makes bundle design central to contract performance.

I begin by examining whether firms comply with quality targets. Credible estimates of compliance are scarce, as counterfactual contract designs are rarely observed within the same market. I use the staggered introduction of stricter quality targets across 30% of routes in the 2022 Transantiago contract redesign to evaluate firm behavior. I find that firms adhere closely to frequency targets but deviate substantially from regularity targets, which suggests that the cost of improving regularity exceeds the penalties for failing to meet it. However, stricter targets do alter behavior: frequency rises by about 5%, consistent with firms already being near compliance, while regularity rises by 17.5%, generating reductions in wait times and improvements in service quality. In other words, while regularity is underprovided under baseline enforcement, tightening the targets produces gains that translate into wait time reductions. Finally, travelers respond to these service improvements, with ridership increasing by 7.5% on treated routes relative to control routes.

These facts demonstrate that both quality target responses and network fragmentation are central to the functioning of this market. To quantify their welfare implications and

evaluate the performance of counterfactual contract designs, I develop and estimate a model of public transportation outsourcing. The model has two components: a demand side, where I estimate traveler preferences from revealed mode and route choices, and a supply side, where I estimate operator cost parameters from revealed preferences in service attribute choices under the 2022 Transantiago contract reform.

On the demand side, I estimate travel preference parameters for in-vehicle travel time, wait time, fares, and transfer penalties using maximum likelihood estimation of travelers' mode and route choices, following Kreindler *et al.* (2023). This component of the model captures complementarities across routes and the welfare gains from quality improvements. On the supply side, I estimate operator cost parameters from firms' profit-maximizing first-order conditions to identify labor elasticity, quality elasticity, and economies-of-scale parameters. This component captures the trade-offs firms face in meeting stricter quality targets and the efficiency gains that can arise from bundling.

Using these estimates, I first examine how market structure affects welfare in the absence of regulation. A monopoly sets higher fares and underprovides quality, but coordinates operations across the entire network. Adding more firms introduces competition on prices but fragments the network, which increases externalities. In my simulations, I find that consumer surplus rises only modestly and producer surplus falls only gradually as the number of firms grows. This pattern reflects an important nuance: because the bundles I simulate isolate firms in nearly disjoint geographic areas, competition does not fully materialize, and each firm retains local market power. As a result, prices do not decline as much as theory might predict, and externalities from fragmentation eventually dominate, lowering welfare at higher levels of competition.

I then evaluate the performance of quality targets, which represent the main regulatory tool currently in place. These targets penalize firms for underperforming on service attributes and can, in theory, push provision closer to the social optimum. In my simulations, quality targets substantially reduce externalities and improve passenger experience, but they do not alter firms' ability to charge prices above cost. The outcome resembles a set of local monopolies that are disciplined on quality but not on prices, so welfare improves relative to the unregulated case but remains far from the planner's benchmark.

Finally, I consider the role of route bundling, which determines how competition unfolds. The current bundling design generates local monopolies that limit the effectiveness of competition, which explains why producer surplus remains high even as more firms enter. My framework suggests that alternative bundling strategies—by mixing routes across geographic areas—could enhance competition and reduce local market power. Importantly, this policy would complement quality targets by addressing different market failures: bundling would discipline prices, while targets would discipline quality. Together,

they have the potential to bring market outcomes much closer to the social planner's benchmark, though the design must balance stronger competition against the risk of further fragmentation.

Related literature This paper contributes to the growing literature on the design and evaluation of public transit policies. Existing work has highlighted the role of subsidies, fare regulation, and network design in shaping ridership and welfare (Barwick *et al.*, 2021; Almagro *et al.*, 2022; Kreindler *et al.*, 2023; Wang, 2024). Other studies emphasize the consequences of private provision in less regulated settings, such as minibus markets in developing country settings (Conwell, 2023; Mbonu and Eaglin, 2024). By focusing on how quality targets and bundling rules affect both operations and tendering outcomes, I add a new perspective to this literature. The evidence from Santiago shows that contract design can alter firms' incentives in ways that matter for service quality, passenger behavior, and overall welfare. My results suggest that policy instruments often treated as secondary to pricing and subsidies can play a central role in aligning private provision with social objectives.

The paper also relates to the broader literature on private participation in the provision of public services. A large body of work has studied how privatization and outsourcing affect efficiency, quality, and access in sectors such as water, electricity, and health. A central theme in this research is the tension between harnessing competition and safeguarding service quality, particularly when performance is hard to monitor or contracts are incomplete. My analysis contributes to this debate by showing how contract design in public transit can manage these trade-offs. Stricter quality targets improved reliability but raised costs, while route reassignment increased competition but fragmented the network. This highlights the importance of institutional design in balancing efficiency with consumer protection in regulated service industries.

Finally, this paper builds on the growing use of structural models to study transportation industries. Recent work has applied such approaches to analyze the behavior of taxi drivers (Buchholz, 2022; Frechette *et al.*, 2019), the organization of trucking and shipping networks (Brancaccio *et al.*, 2020), and competition in railroads and airlines (Chen, 2024; Degiovanni and Yang, 2023; Yuan and Barwick, 2024). These studies show how market structure and firm behavior interact with regulation and infrastructure to shape welfare outcomes. My contribution is to extend this framework to urban bus transit, a sector where contracting and regulation rather than direct pricing are the main levers of policy. By combining reduced-form evidence with a structural model disciplined by the data, I am able to quantify the welfare effects of alternative contract designs and provide a counterfactual benchmark for policy evaluation.

2 Theoretical Framework

In this section, I present a theoretical framework for optimal regulation of transit service provision in the presence of market power, externalities, and network effects. As a key departure from the literature on transportation regulation under market power, firms in this model respond to government policies by adjusting both prices and service attributes of their route networks. This framework enables me to characterize the welfare implications of two policy instruments: quality targets and competitive route bundling mechanisms.

The framework involves N differentiated transit routes, indexed by j , each characterized by a K -element service attribute vector $x_j = (x_j^1, x_j^2, \dots, x_j^K)$ (e.g., frequency, regularity) and price P_j . Route j generates external benefits $e_j(x_j) > 0$ due to reductions in pollution and traffic congestion externalities when travelers shift from more externality-intensive transportation modes. Both consumer willingness-to-pay $B_j(x)$ and the marginal cost of service provision $C_j(x_j)$ depend on service attributes, where $x = (x_1, \dots, x_N)$ captures network effects arising from the interdependence of route choices.

Throughout the theoretical analysis, I assume that consumer demand exhibits additive separability between price disutility and service attributes: $Q_j(P, x) = Q_j(P_j - B_j(x))$. This demand function is motivated by discrete choice models where utility depends on prices and attributes additively. Following Barwick *et al.* (2024), the additive separability makes firms' choices of prices and attributes independent and greatly simplifies the model. Most importantly, it enables me to characterize optimal policy design in the presence of market power and network externalities, which has not been done in the transit regulation literature. A limitation of the additivity assumption is that the marginal value of service attributes is the same across consumers, which rules out the Spence distortion in quality provision.

The theoretical analysis compares the privately and socially optimal outcomes and discusses the choice of regulatory instruments to rectify market failures in transit provision. To build intuition, I first analyze the baseline case of a social planner before examining monopoly provision without regulation, then extending to quality regulation and competitive bundling mechanisms.

2.1 Social Planner

The social planner maximizes social welfare that consists of consumer surplus, producer surplus, and externalities. Consider a social planner that chooses prices and service

attributes to maximize social welfare:

$$\max_{P,x} \quad SW(P,x) = \sum_{j=1}^N \left[\underbrace{\int_0^{Q_j(P,x)} \left(B_j(x) + Q_j^{-1}(s) - P_j \right) ds}_{\text{Consumer surplus}} \right. \\ \left. + \underbrace{(P_j - C_j(x_j)) Q_j(P,x)}_{\text{Producer surplus}} + \underbrace{\phi \cdot e_j(x_j) Q_j(P,x)}_{\text{Externality}} \right] \quad (1)$$

The socially optimal prices P_j^* and service attributes x_j^* satisfy the following first-order conditions:

$$[P_j] : \quad P_j^* - C_j(x_j^*) + \phi \cdot e_j(x_j^*) = 0 \quad (2)$$

$$[x_\ell^i] : \quad \underbrace{\left[\frac{\partial B_i(x^*)}{\partial x_\ell^i} - \frac{\partial C_i(x_i^*)}{\partial x_\ell^i} + \phi \cdot \frac{\partial e_i(x_i^*)}{\partial x_\ell^i} \right] Q_i}_{\text{Direct effect on route } i} + \underbrace{\sum_{j \neq i}^N \left[\frac{\partial B_j(x^*)}{\partial x_\ell^i} Q_j \right]}_{\text{Network effect}} = 0 \quad (3)$$

The first-order conditions reflect that service attributes are chosen to maximize per-unit social surplus, $B_j(x) - C_j(x_j) + \phi \cdot e_j(x_j)$, while prices reflect the social cost of service provision, $C_j(x_j^*) - \phi \cdot e_j(x_j^*)$. The socially optimal price P_j^* eliminates quantity distortions, while the socially optimal attributes x_j^* internalize both environmental externalities and network effects across routes.

2.2 Monopoly without Regulation

Consider a monopolist that controls the entire transit network and chooses prices and service attributes to maximize profit:

$$\max_{P,x} \quad \Pi(P,x) = \sum_{j=1}^N [(P_j - C_j(x_j)) Q_j(P,x)] \quad (4)$$

The privately optimal prices P_j^m and service attributes x_j^o satisfy:

$$[P_j] : \quad \frac{P_j^m - C_j(x_j^o)}{P_j^m} = \frac{1}{\varepsilon_{P_j}} \quad (5)$$

$$[x_\ell^i] : \underbrace{\left[\frac{\partial B_i(x^o)}{\partial x_\ell^i} - \frac{\partial C_i(x_\ell^o)}{\partial x_\ell^i} \right] Q_i}_{\text{Direct effect on route } i} + \underbrace{\sum_{j \neq i}^N \left[\frac{\partial B_j(x^o)}{\partial x_\ell^i} Q_j \right]}_{\text{Network effect}} = 0 \quad (6)$$

where ε_{P_j} is the price elasticity of demand for route j . The first-order conditions differ from Equations (2) and (3) in three important ways.

First, the monopolist sets $P_j^m > P_j^*$, resulting in underprovision of quantity relative to the social optimum due to markup pricing under downward-sloping demand. Second, the monopolist does not internalize external benefits $\phi \cdot e_j(x_j)$, leading to inefficient service quality choices where routes may be under-served in terms of environmentally beneficial attributes. Third, while the monopolist controls all routes and thus internalizes network effects through the term $\sum_{j \neq i} \frac{\partial B_j(x^o)}{\partial x_\ell^i} Q_j$, it chooses suboptimal attribute levels because it ignores externalities. Consequently, it does not generate the full social value of network coordination that would justify higher service levels.

2.3 Monopoly with Quality Regulation

Suppose the government introduces quality targets \bar{x}_j for each route j to address externality distortions. To incentivize compliance, the firm faces penalties when deviating from these targets:

$$\mathcal{P}_j(x_j, \bar{x}_j) = \tau \cdot s_j(x_j, \bar{x}_j),$$

where $\tau > 0$ is a penalty strength parameter and $s_j(\cdot)$ represents the penalty function. The regulated monopolist maximizes:

$$\max_{P, x} \Pi(P, x) = \sum_{j=1}^N [(P_j - C_j(x_j) - \tau \cdot s_j(x_j, \bar{x}_j)) Q_j(P, x)] \quad (7)$$

The regulated equilibrium prices P_j^z and service attributes x_j^z satisfy:

$$[P_j] : \frac{P_j^z - C_j(x_j^z) - \tau \cdot s_j(x_j^z, \bar{x}_j)}{P_j^z} = \frac{1}{\varepsilon_{P_j}} \quad (8)$$

$$[x_\ell^i] : \underbrace{\left[\frac{\partial B_i(x^z)}{\partial x_\ell^i} - \frac{\partial C_i(x_\ell^z)}{\partial x_\ell^i} - \tau \cdot \frac{\partial s_i(x_\ell^z, \bar{x}_i)}{\partial x_\ell^i} \right] Q_i}_{\text{Direct effect on route } i} + \underbrace{\sum_{j \neq i}^N \left[\frac{\partial B_j(x^z)}{\partial x_\ell^i} Q_j \right]}_{\text{Network effect}} = 0 \quad (9)$$

Quality regulation addresses externality distortions but leaves market power intact. The monopolist continues to set $P_j^z > P_j^*$, leading to underprovision of quantity relative to the social optimum, as the penalty function affects profit levels but not marginal pricing incentives. However, if the marginal penalty equals the marginal externality:

$$\tau \cdot \frac{\partial s_j(x_j, \bar{x}_j)}{\partial x_\ell^j} = \phi \cdot \frac{\partial e_j(x_j)}{\partial x_\ell^j} \quad \text{for all } j, \ell,$$

then the regulated monopolist chooses efficient service quality levels: $x_j^z = x_j^*$. Under this condition, the monopolist also internalizes the full network benefits that a social planner would, since it controls all routes and quality incentives are properly aligned.

2.4 Competitive Route Bundling

I now introduce a two-stage mechanism where competition occurs via auctions over packages of transit routes, followed by decentralized service provision by winning firms. This mechanism addresses market power distortions while potentially affecting the internalization of network effects.

The N transit routes are partitioned into B disjoint packages $\mathcal{R}_b \subset \{1, \dots, N\}$. In the first stage, firms $k \in \mathcal{K}$ submit bids P_{kb} representing the per-passenger price they would charge for operating bundle b . The regulator awards each bundle to the lowest bidder:

$$k(b) = \arg \min_{k \in \mathcal{K}} P_{kb}.$$

In the second stage, each winning firm chooses service attributes x_j for routes $j \in \mathcal{R}_b$ to maximize profit, taking prices as given from the auction outcome.

2.4.1 First-Stage Bidding

In the auction stage, firm k chooses bid P for bundle b to maximize expected profit. Assuming symmetric firms with i.i.d. rival bids following distribution $F(\cdot)$, the probability of winning with bid P is $(1 - F(P))^{n-1}$, where n is the number of bidders. Expected profit is:

$$\max_P \quad (1 - F(P))^{n-1} \cdot \pi_k(P),$$

where $\pi_k(P) = \sum_{j \in \mathcal{R}_b} \left(P - C_j(x_j^{auction}) \right) Q_j$.

The first-order condition for optimal bidding yields:

$$\sum_{j \in \mathcal{R}_b} \left[(P_b - C_j(x_j^{auction})) \cdot \frac{\partial Q_j}{\partial P} + Q_j \right] = (n-1) \cdot \pi_k(P_b) \cdot \frac{f(P_b)}{1 - F(P_b)} \quad (10)$$

This condition balances the marginal profit from raising the bid (left side) against the increased probability of losing the auction (right side). As competition intensifies (n increases), the equilibrium bid P_b decreases toward marginal cost, addressing the quantity distortion from market power.

2.4.2 Second-Stage Service Provision

After winning bundle b , firm k chooses service attributes to maximize profit given the auction-determined price P_b :

$$\max_{x_j; j \in \mathcal{R}_b} \sum_{j \in \mathcal{R}_b} [(P_b - C_j(x_j)) \cdot Q_j(P_b, x)].$$

The optimal service attributes satisfy:

$$[x_\ell^i] : \underbrace{\left[\frac{\partial B_i(x^{auction})}{\partial x_\ell^i} - \frac{\partial C_i(x^{auction})}{\partial x_\ell^i} \right] Q_i}_{\text{Direct effect on route } i} + \underbrace{\sum_{j \in \mathcal{R}_b, j \neq i} \left[\frac{\partial B_j(x^{auction})}{\partial x_\ell^i} Q_j \right]}_{\text{Within-bundle network effect}} = 0 \quad (11)$$

Comparing Equation (11) with (3) reveals that competitive bundling internalizes network effects only within each bundle \mathcal{R}_b , but not across bundles operated by different firms. The mechanism eliminates externality distortions only if combined with appropriate quality regulation, and the efficiency of network effect internalization depends critically on how routes are grouped into bundles.

2.5 Discussion

My theoretical framework illustrates the distinct roles of quality regulation and competitive bundling in addressing market failures in transit provision. Quality targets can eliminate externality distortions and restore efficient network coordination when properly calibrated, but leave market power intact. Competitive bundling addresses market power through price competition but may fragment network coordination depending on bundle design. The optimal regulatory approach depends on the relative importance of these distortions and the administrative feasibility of different policy instruments, questions I address empirically in the next sections.

3 Background and Institutional Setting

My empirical setting is Santiago's public transit system, Transantiago, which uses contract-based provision of urban bus services and it is administered by the *Directorio de Transporte*

Público Metropolitano (DTPM). Since its launch in 2007, Transantiago has delegated operation of its 373 bus routes—served by a fleet of 6,550 buses—to private firms through competitively tendered contracts, while the subway system remains publicly operated. The fare-integrated network serves 3.5 million daily trips across a metropolitan area of 7 million people, with annual budget exceeding US\$1.1 billion. Transantiago is among the largest and most mature examples of bus contracting globally, making it an interesting case for studying how contract design affects service provision in regulated markets. Its relevance has grown as cities such as Singapore, Paris, and Hong Kong have adopted similar models, increasing interest in the design of incentives and oversight in transit systems.

3.1 Tendering

Unlike fixed-price or cost-plus contracts, DTPM allocates bus service contracts through a competitive scoring auction that creates ex-ante competition among private operators. Firms submit bids for contracts that specify bundles of bus routes, each linked to a designated set of bus depots controlled by DTPM. Depot proximity facilitates efficient operations, while capacity constraints limit the feasible combinations of routes that can be assigned to a given location.

Each bid includes two key decision variables: the per-kilometer price the firm is willing to accept and the fleet size it proposes to operate the bundle. These economic components are scored alongside technical criteria—such as the firm’s experience in urban transit, proposed fleet characteristics, and compliance with formal requirements—using a transparent scoring rule in which the economic score receives 80–90% of the total weight. At the time of bidding, firms observe historical ridership, the depot assignment for each bundle, the regulator-set per-passenger price, and the penalty structure that governs performance monitoring. These auction-stage choices shape both the firm’s expected profits and its operational incentives under the contract. In my structural model, I treat the price and fleet size as the firm’s decision variables at the tendering stage.

3.2 Operations

Beyond the auction stage, Transantiago’s contract structure creates ongoing incentives for firms to determine how to operate their assigned routes. Firms receive revenue from two sources: a per-passenger payment set by DTPM and a per-kilometer payment determined by their bid. To earn the latter, firms must actively deploy service—i.e., dispatch vehicles to cover the planned kilometers—making service frequency a choice variable. In addition to frequency, firms also choose how evenly to space vehicle departures, as regulators monitor the regularity of headways on each route. Both frequency and regularity affect traveler waiting times and are central to the system’s service quality targets.

DTPM monitors these attributes using GPS data transmitted from each bus every 30 seconds. Monitoring is conducted within predefined periods (e.g., 30 min, 60 min, 120 min), and financial penalties are applied when firms deviate from route-level frequency or regularity targets. These penalties are determined by publicly known functions written into each contract and directly reduce firms' revenues. As a result, the auction outcomes—specifically, the per-kilometer price and fleet size—interact with operational choices made during the contract period. In my structural model, I explicitly treat frequency and regularity as firm-level decision variables shaped by these contractual incentives.

4 Data

My empirical analysis combines several administrative and survey datasets to study how transit contract design affects service provision, bidding behavior, and travel decisions. This section describes each dataset and how I use it in the analysis.

4.1 Mode and Route Choices

I combine individual travel choices from the 2012–2013 Household Travel Survey with reconstructed trip attributes based on operational data from the same period. The survey records all daily trips made by approximately 60,000 individuals across 18,000 randomly sampled households in the Santiago metropolitan area. The sample is representative at a fine geographic level across 866 origin-destination zones averaging 1 km² in size. I restrict attention to the 700 urban zones, which account for nearly 50,000 urban trips and cover 80% of work-related trips and 83% of the city's residential population.

For each trip, I observe origin and destination coordinates, traveler demographics (income, car ownership, age, gender, education), and the chosen mode (car, public transit, walking, or other). Figure C.2a shows the distribution of mode choices by income group, revealing substantial heterogeneity in travel patterns: high-income travelers use cars for 68% of trips compared to only 21.8% for low-income travelers. For car trips, I compute monetary costs using fuel prices and maintenance costs from the *Comisión Nacional de Energía de Chile*, assuming an average fuel economy of 8.3 km/liter.¹ I obtain travel times and distances using the OSRM routing engine based on OpenStreetMap data, using the exact origin and destination coordinates from the survey.

For public transit trips, the survey identifies the exact bus and metro routes used in each leg. However, it does not report leg-level attributes such as fare, travel time, distance,

¹Fuel economy source: https://energia.gob.cl/sites/default/files/documentos/20240304_informe_final_estandar_-_vehiculos_medianos_vf.pdf

or frequency. To recover these, I use DTPM’s trip reconstruction algorithm, developed by Munizaga and Palma (2012), which combines GPS and smartcard data to reconstruct complete transit itineraries and their characteristics.² This allows me to merge observed survey trips with corresponding travel time, distance, and frequency for representative weeks in 2012 and 2013. I obtain fares separately from administrative fare tables published by DTPM for the corresponding period.

I successfully match 23,400 out of 27,000 public transit trips in the survey to operational data, enabling the construction of a rich dataset of individual travel choices linked to detailed service characteristics across all main transport modes. The resulting data reveals clear trade-offs in route choice, as illustrated in Figure C.2b, where faster travel speeds are associated with longer wait times, particularly distinguishing between direct transit routes and those requiring transfers. I use this dataset to estimate travel preference parameters in the structural model.

4.2 Frequency and Headway Regularity Choices

I use GPS data from DTPM covering the entire Transantiago bus network between August 2022 and August 2023. Each vehicle transmits its location every 30 seconds, and the dataset includes the route, operator, vehicle ID, timestamp, and coordinates. These data are used by DTPM for contract monitoring and penalty enforcement, and achieve full coverage across all firms, routes, and days. I am not aware of any gaps or missing vehicles during the observation window.

I construct two key service attributes that enter the firm’s decision problem in my structural model of the Operations stage. First, frequency measures the number of vehicle dispatches per route within a monitoring period. Monitoring periods vary in length across contracts but generally span between 30 minutes and 3 hours. Second, regularity captures the consistency of headways between consecutive buses, computed as the coefficient of variation within each monitoring period. Both dimensions shape user waiting times and are directly incentivized by contract enforcement rules. Figure C.3 illustrates these concepts using representative GPS trajectories and shows how firms make strategic trade-offs between frequency and regularity.

For estimation, I aggregate these measures to the route-day level, excluding night service (12am–5am) and dispatches flagged by DTPM as exempt from performance evaluation. This yields a panel of 549,000 route-day observations, balancing data

²The algorithm uses all transit card transaction data to reconstruct individual trips. For each card, it matches tap-in times with GPS vehicle locations to infer trip origin, route legs, leg-level travel times, and service attributes such as frequency and regularity. Since users do not tap out, destinations are imputed based on weekly travel patterns, assuming reciprocal morning and evening origins. DTPM reports that the method matches approximately 25 million trips per week, consistent with system-wide tap-in volumes.

consistency with institutional variation in monitoring periods across contracts.

4.3 Equilibrium Outcomes: Travel Time, Traffic Flow, and Ridership

First, I measure public transit ridership using smartcard transaction data that record all system tap-ins. These data provide route-level boardings in 30-minute intervals for every day in the observation period, covering approximately 3.5 million trips per weekday. I use these data to examine whether more stringent quality targets increase ridership at the route level.

Second, I use vehicle count data from 70 automatic traffic sensors distributed across major corridors in Santiago. These sensors record vehicle flows in 15-minute intervals and provide citywide coverage of key traffic arteries. I complement these data with travel speed information from Google Maps API, matched to the same locations and timestamps. These traffic and speed data span the period from August 1 to September 17, 2022, and were originally collected by Bordeu (2023) using sensors maintained by the Chilean Ministry of Transportation.

Figure C.4 illustrates relationships in these data: Panel (a) shows the traffic flow-speed relationship that underlies the road technology, while Panel (b) demonstrates the association between transit service reliability and ridership demand.

I use this combination of traffic flow and speed data to estimate a road technology model that maps vehicle flows to travel times. This relationship allows me to predict how equilibrium travel speeds adjust when transit service quality or car usage changes endogenously in the model.

5 Descriptive Evidence

At the end of 2022, DTPM launched a major contract retendering process that reassigned more than 40% of routes due to the expiration of 5–7 year contracts. The reform introduced two contract design changes. First, quality targets were made more stringent by standardizing monitoring periods from irregular 2–3 hour intervals to uniform 30-minute windows, increasing the strength of enforcement. Second, several large route bundles were divided into smaller ones, altering the degree of network fragmentation across operators. Because route eligibility for retendering was determined by predetermined contract cycles, these changes provide plausibly exogenous variation in contract design across routes and operators.

These contract modifications affected firms asymmetrically: some operators lost most of their routes, others retained a subset, and at least one preserved their full network. This heterogeneity generates distinct sources of variation that can be used to

examine the effects of contract design on service outcomes. In this section, I present descriptive evidence along two margins. First, I study how stricter quality targets affected firms' provision of frequency and headway regularity, as well as the induced ridership response. Second, I analyze how network fragmentation—shaped by bundle size and operator assignment—affects market power and coordination across routes within origin-destination trips. These reduced-form results provide evidence on the mechanisms through which contract design influences service quality and passenger welfare, and they motivate the structural analysis that follows.

5.1 Effect of Quality Targets on Service Attributes

Figure 1 illustrates deviations from planned service attributes in the pre-reform period (August to December 2022). Firms closely adhered to frequency targets, with bunching around zero deviation, but systematically deviated from headway regularity targets by providing more irregular dispatches. This pattern suggests that the monetary penalties for non-compliance were less costly than achieving stricter regularity, leading firms to tolerate penalties rather than invest in coordination. To test whether tighter quality targets can shift this trade-off, I exploit the introduction of more stringent monitoring rules during contract retendering.

Empirical Strategy In late December 2022, 40% of routes were reassigned through the expiration of 5–7 year contracts. Retendered contracts introduced stricter quality targets by standardizing monitoring periods from irregular 2–3 hour windows to uniform 30-minute intervals, thereby strengthening enforcement of service regularity. Because route eligibility was determined by predetermined contract cycles, treatment assignment is plausibly exogenous to contemporaneous performance. The staggered implementation across routes allows for an event study design.

I estimate the following specification:

$$\log(y_{rdkt}) = \sum_{l \neq -1} \beta_l \text{Treated}_r \cdot \mathbb{1}\{t = l + 1\} + \mu_r + \lambda_k + \delta_t + X'_{rt} \phi + \varepsilon_{rdkt}, \quad (12)$$

where y_{rdkt} denotes service outcomes for route r operated by firm k from depot d on day t . I focus on frequency, headway regularity (coefficient of variation), and passenger ridership. Treated_r is an indicator for routes subject to stricter quality targets. The specification includes route fixed effects (μ_r), firm fixed effects (λ_k), and date fixed effects (δ_t). X_{rt} controls for time-varying route characteristics such as length and average speed. Standard errors are clustered at the firm level. The sample spans August 2022 to August 2023.

Results Figure 2 plots the event study estimates. The results show heterogeneous responses across service attributes, consistent with the compliance patterns observed pre-reform. For frequency, stricter quality targets produce a modest increase of about 5%, reflecting that firms were already largely meeting frequency requirements. In contrast, the effect on regularity is much larger: stricter targets reduce the coefficient of variation of headways by 17.5%, a substantial improvement in scheduling consistency. Finally, when ridership is used as the outcome, treated routes experience a 7.5% increase in passenger demand relative to controls. All effects are statistically significant at the 1% level, emerge immediately after implementation, and remain stable throughout the post-reform period.

Discussion The results indicate a two-step mechanism through which stricter quality targets improve service and passenger welfare. First, firms respond to enhanced enforcement by improving the attribute where non-compliance was most common: headway regularity. The sharp decline in headway variation shows that firms had the operational capacity to provide more regular service but lacked incentives to do so under the previous, weaker penalty structure. Second, passengers respond positively to these improvements, as reflected in higher ridership, suggesting that coordination generates significant welfare gains.

The modest frequency response versus the large regularity improvement highlights an important trade-off in service provision. Frequency can be adjusted with relatively minor cost changes, but improving regularity likely requires investments in coordination systems, driver scheduling, and operational oversight that are not directly observed in the data. That firms undertake these adjustments under stricter enforcement suggests that the welfare gains from better coordination exceed these private costs. Quantifying this trade-off requires a structural framework that can capture the cost structure of quality provision and assess how alternative contract designs balance welfare gains from stricter quality targets against the associated cost increases.

5.2 Effect of Network Fragmentation on Service Attributes

Figure 3 provides a visual example of network fragmentation. When routes that previously belonged to the same operator are reassigned to different operators, the network becomes fragmented. This reallocation could limit the ability of operators to coordinate headways across routes, potentially worsening regularity and increasing passenger waiting times. To formally test this hypothesis, I relate variation in market concentration, measured by the Herfindahl–Hirschman Index (HHI), to observed service quality outcomes in the pre-reform period.

Empirical Strategy To examine the relationship between network fragmentation and service quality, I restrict attention to the pre-reform period (August to December 2022) in order to avoid confounding effects from the change in quality targets that began at the end of 2022. For each trip reported in the household travel survey and each day in this period, I construct the relevant route choice set. Each choice set includes all feasible routes and their observed attributes: operator identity, observed frequency, headway regularity (measured as the coefficient of variation of headways), and expected wait time.

To measure network fragmentation, I compute the market share of each route within a trip–OD–date choice set. I construct the market share using the planned frequency of the route (which is predetermined by contract and not a firm decision). Using these shares, I compute the Herfindahl–Hirschman Index (HHI) of concentration at the trip–OD–date level. The resulting panel dataset allows me to relate variation in market concentration to service attributes.

I estimate the following regression specification:

$$\log(y_{itod}) = \beta \log(\text{HHI}_{itod}) + \alpha_i + \alpha_t + \alpha_o + \alpha_d + X'_{itod} \gamma + \varepsilon_{itod}, \quad (13)$$

where y_{itod} denotes one of three outcome variables (aggregate frequency, aggregate coefficient of variation of headways, or expected wait time) for trip i , origin o , destination d on date t . The specification includes fixed effects for trip (α_i), date (α_t), origin (α_o), and destination (α_d), and standard errors are clustered at the traveler level. X_{itod} includes total planned frequency and the number of routes in the market as controls.

Results Table 1 presents the regression estimates. The coefficient of interest is the elasticity of service outcomes with respect to market concentration, measured by the Herfindahl–Hirschman Index (HHI). In column (1), I find that a 10% increase in HHI is associated with a 1.38% reduction in aggregate frequency. In column (2), the same 10% increase in HHI leads to a 2.24% reduction in the coefficient of variation of headways, indicating improved regularity. Finally, in column (3), a 10% increase in HHI reduces expected waiting time by 0.27%. Taken together, these results suggest that higher market concentration decreases service frequency but improves headway coordination, with the latter effect dominating to slightly reduce expected wait times on net. The estimates are precise, and all effects are statistically significant at the 1% level.

Discussion The results highlight two distinct channels through which network fragmentation affects service quality. On the one hand, higher concentration reduces aggregate service frequency. This suggests that dominant firms may exercise market power by reducing costly service provision. On the other hand, an increase in concentration lowers

the coefficient of variation of headways. This pattern is consistent with the idea that fragmented markets suffer from poorer coordination across operators, while concentrated markets can better schedule departures to avoid bus bunching. Finally, the wait time reductions suggest that the coordination effect slightly dominates the frequency effect in terms of passenger outcomes. In other words, the efficiency gains from more regular headways are just strong enough to offset the loss of frequency. This provides suggestive evidence that in this setting, coordination externalities are quantitatively important and can partially mitigate the service quality losses associated with market power. These findings motivate the counterfactual analysis using a structural model, where I examine how alternative contractual instruments—such as bundling routes under common operators or enforcing stricter quality targets—can influence the balance between market power and network effects.

6 Empirical Model

The reduced-form analysis confirms that contract parameter changes affect service quality and ridership patterns. To evaluate the welfare implications of different contract designs and to quantify the underlying mechanisms driving these effects, I now turn to an equilibrium model that features three key economic agents: travelers making mode and route choices, private transit operators making service attribute decisions, and a transit agency designing the contractual environment.

The model characterizes the interactions between travel demand and transit service provision in a regulated oligopolistic environment. On the one hand, travelers' mode and route choices determine ridership patterns, which affect operators' revenues and hence their incentives for service provision. On the other hand, operators' choices on service attributes—particularly frequency and headway regularity—directly affect the attractiveness of different travel options through travelers' wait times, and therefore consumer surplus. The equilibrium nature of my model allows counterfactual simulations of different contract designs and provides direct comparative statics of service quality, ridership, traffic congestion, and social welfare across policy alternatives.

My approach addresses a gap in the existing literature on transit regulation, which has primarily focused on either completely decentralized markets (e.g., minibuses in African cities) or public monopolistic provision (e.g., transit systems in US cities or BRTs in developing countries). No previous study has examined a regulated oligopolistic environment where service provision is delegated to private firms operating under performance contracts with quality targets and competitive route bundling mechanisms.

The model assumes that travelers' origins and destinations are determined *ex ante*

and examines mode and route choices given these fixed trip patterns. This assumption is motivated by three considerations. First, for most urban trips, origins and destinations reflect longer-term residential and employment decisions that respond slowly to transportation policy changes. Second, the contract parameter variation I exploit occurred over a relatively short time horizon, making it unlikely that fundamental location patterns adjusted significantly. Third, incorporating joint location-transportation choices would substantially complicate the empirical analysis given the rich individual-level preference heterogeneity I incorporate into the model.

My approach offers several methodological advantages over existing studies of transportation policy. First, my rich operational data on service attribute decisions allows me to estimate cost parameters directly from observed operator choices rather than relying solely on auction bids, which is important given the limited bidding data available in my setting. Second, the discrete route choice framework enables me to decompose travelers' expected utility from transit into direct effects (utility from the chosen route) and network effects (utility from having other routes as alternatives), providing novel insights into the welfare consequences of network fragmentation under competitive bundling.

The model has limitations that I acknowledge. I abstract from dynamic considerations and treat the analysis as a static equilibrium. I assume travelers' origins, destinations, and the physical route network are fixed, focusing on how existing routes can be reallocated across different operators rather than network redesign. I model road congestion affecting car travel times but abstract from crowding effects on transit vehicles. Finally, I focus on the three dominant transportation modes (car, public transit, walking) and abstract from smaller-share alternatives like taxis and ride-sharing services.

6.1 Travelers

I model travelers as making decisions in two sequential stages: first choosing among transportation modes, then, conditional on selecting public transit, choosing among available routes. This two-stage structure captures not only substitution among transportation modes but also substitution among transit routes in response to endogenous service attributes that reflect transit operators' responses to contract design.

6.1.1 Stage 1: Mode Choice

For a given origin-destination pair (market m), traveler i 's utility from choosing mode j is given by:

$$u_{ijm} = \theta_{ij} + v_{jm} + \chi_{jm} + \epsilon_{ijm} \quad (14)$$

where θ_{ij} is a mode-specific random coefficient that varies across individuals, v_{jm} is the deterministic utility component, χ_{jm} represents observable mode-market characteristics, and ϵ_{ijm} is an idiosyncratic error term assumed to follow a Type I extreme value distribution.

The choice set includes three transportation modes: car, public transit, and walking (the outside option). Mode availability depends on individual circumstances and infrastructure access. For car availability, the Household Travel Survey data indicates whether individuals have access to a vehicle. For transit accessibility, I identify all bus stops and subway stations within 1,000 meters of both trip origins and destinations, determining the set of transit routes serving these access points.

The deterministic utility component v_{jm} varies by transportation mode:

$$v_{jm} = \begin{cases} \mathbb{E} \max_{r \in \mathcal{R}_m} u_{rm}, & \text{if } j = \text{transit} \\ \alpha_{\text{price}} P_{jm} + \alpha_{\text{veh}} T_{jm}^{\text{veh}}, & \text{if } j = \text{car} \end{cases} \quad (15)$$

For car travel, the deterministic utility depends on trip cost P_{jm} and travel time T_{jm}^{veh} . Trip costs include both fuel expenses and maintenance costs.³ For public transit, the deterministic utility equals the expected maximum utility across all available routes \mathcal{R}_m in market m , which I discuss in Section 6.1.2, where I provide details of the route choice model. Walking serves as the outside option with utility normalized to zero, ensuring model identification and providing a baseline for comparing other transportation modes.

The observable characteristics χ_{jm} include three sets of fixed effects interacted with mode indicators. First, I include mode-specific fixed effects to capture average preferences across transportation options. Second, I incorporate mode-trip characteristic interactions, where trip variables include distance, purpose, time period, and indicators for whether trips originate or terminate in the central business district. Third, I include mode-demographic interactions with traveler characteristics including education, age, and gender.

Individual heterogeneity enters through the mode-specific random coefficient θ_{ij} , which allows baseline preferences for each transportation mode to vary across travelers. This specification maintains tractability while capturing unobserved preference heterogeneity that affects mode choice decisions.

³Fuel expenses are calculated as the product of distance, fuel efficiency, and gasoline prices. Maintenance costs are calculated as the product of distance and by per-kilometer maintenance rates

Choice Probabilities Given the Type I extreme value distribution assumption for ϵ_{ijm} , the probability that traveler i chooses mode j in market m follows a standard logit specification:

$$\mathbb{P}_{ijm} = \frac{\exp(\theta_{ij} + v_{jm} + \chi_{jm})}{\sum_{k \in J_m} \exp(\theta_{ik} + v_{km} + \chi_{km})} \quad (16)$$

where J_m represents the set of available modes in market m .

6.1.2 Stage 2: Transit Route Choice

The traveler chooses among transit route options $h \in \mathcal{H}_m$ in market m (origin-destination pair). Building on the model developed by Kreindler *et al.* (2023), each option h consists of either a direct route r or a combination of two routes r_1 and r_2 connected through a transfer. The utility from option h depends on a deterministic component and a random wait time component:

$$u_h = v_h + \alpha_{\text{wait}} T_h^{\text{wait}} \quad (17)$$

This model assumes that bus arrivals on route r follow a Poisson process with arrival rate λ_r . This generates exponentially distributed wait times with the property that $\Pr(T_r^{\text{wait}} > w) = \exp(-\lambda_r w)$.

The deterministic utility component v_h is given by:

$$v_h = \begin{cases} \alpha_{\text{price}} P_h + \alpha_{\text{veh}} T_h^{\text{veh}}, & \text{if } h = \text{Direct} \\ \alpha_{\text{price}} P_h + \alpha_{\text{veh}} T_{r_1}^{\text{veh}} \\ \quad + \mathbb{E} \max_{r_2} [\alpha_{\text{veh}} T_{r_2}^{\text{veh}} + \alpha_{\text{wait}} T_{r_2}^{\text{wait}}] + \mu_{\text{transfer}}, & \text{if } h = \text{Transfer} \end{cases} \quad (18)$$

P_h is the fare for option h , T_h^{veh} is in-vehicle travel time, T_h^{wait} is wait time governed by the Poisson arrival process, and μ_{transfer} captures the pure disutility of making a transfer.

For direct routes, utility depends on the price, in-vehicle time, and realized wait time for that route. For transfer options, the traveler experiences utility from the first leg (including its wait time) plus the expected utility from optimally choosing among available second-leg routes at the transfer station. This expected utility formulation captures the option value from having multiple connections available at transfer points.

Transit Choice Set I determine route choice sets using detailed origin-destination information from the Household Travel Survey combined with complete network topology data. For each trip, I identify all bus stops and subway stations within 1,000 meters of both origin and destination points. The choice set \mathcal{H}_m for market m includes all direct

routes and single-transfer combinations that connect the accessible origin and destination stations. Choice set sizes vary substantially across markets, with a median of 8 options, ranging from a minimum of 1 to a maximum of 32 available combinations.

Choice Probabilities The exponential wait time assumption yields tractable expressions for choice probabilities and expected utility. The probability of choosing option h among alternatives ranked by deterministic utility $v_1 \leq v_2 \leq \dots \leq v_H$ is:

$$\lambda_h^{-1} \pi_h = \sum_{i=1}^h e^{-\alpha_{\text{wait}}^{-1} M_i} \frac{e^{v_i \alpha_{\text{wait}}^{-1} \Lambda_i} - e^{v_{i-1} \alpha_{\text{wait}}^{-1} \Lambda_i}}{\Lambda_i} \quad (19)$$

where $\Lambda_i = \sum_{j=i}^H \lambda_j$ and $M_i = \sum_{j=i}^H v_j \lambda_j$, with $v_0 = -\infty$ by convention.

This framework ensures computational tractability and avoids the "red bus, blue bus" problem that affects standard logit models, as combining identical routes with split frequencies yields identical choice probabilities and expected utilities.

Expected Utility The expected utility from choosing optimally among available routes is:

$$\mathbb{E} \max_{h \in \mathcal{H}_m} u_h = v_{h^*} - \pi_{h^*} \frac{\alpha_{\text{wait}}}{\lambda_{h^*}} \quad (20)$$

where h^* denotes the option with highest deterministic utility v_{h^*} , π_{h^*} is the probability of choosing option h^* , and λ_{h^*} is its effective frequency (arrival rate). The influence of alternative options $h \neq h^*$ on expected utility is captured through the choice probability π_{h^*} . That is, when more attractive alternatives are available, the probability of choosing any single option decreases, increasing the expected utility from the entire choice set.

Linking Supply Decisions to Arrival Rates The main departure from Kreindler *et al.* (2023) is connecting service attribute decisions to the effective frequency λ_r that determines traveler wait times. Transit operators choose both frequency and headway regularity (measured by the coefficient of variation of headways) for each route r in their bundle.

I model the relationship between these service attribute decisions and travelers' experienced effective arrival rates using the following engineering relationship:

$$\lambda_r = \frac{f_r}{1 + CV_r^2} \quad (21)$$

where f_r is the number of dispatched buses per interval of time and CV_r is the coefficient of variation of headways. When service is perfectly regular ($CV_r = 0$), travelers experience the full dispatched frequency. As service becomes more irregular, the effective frequency

decreases, reflecting longer average wait times due to service bunching and gaps.

This specification captures an important operational trade-off: operators can increase service quality either by running more buses (higher frequency) or by improving service reliability (lower coefficient of variation). The contractual instruments I examine—quality targets and route bundling—affect operators' incentives along both dimensions.

6.2 Private Transit Operators

I model private transit operators as making decisions in two sequential stages: first bidding competitively for bundles of routes in government tenders, then choosing service attributes (frequency and headway regularity) for each route in their awarded bundle. This two-stage structure captures the key trade-offs operators face between service quality and costs, and between regulatory compliance and profit maximization. Crucially, operators make bundle-level decisions that account for both shared depot resources and demand spillovers across routes, enabling them to internalize network effects within their bundle while potentially fragmenting coordination across bundles operated by different firms.

6.2.1 Stage 2: Operations

Each transit firm k operates a bundle of routes \mathcal{R}_k across the depots assigned to the bundle. The firm's operational profit can be expressed as:

$$\Pi_k^{\text{op}} = \text{Revenue}_k - \text{Penalties}_k - \text{Operational Costs}_k \quad (22)$$

This structure captures the central trade-offs between service quality, regulatory compliance, and cost minimization. Now, I detail each component of this profit function.

Revenue Firm revenue comes from two sources, a demand-based and a service-based component. The demand-based component captures passenger revenue:

$$R_{kt}^{\text{pax}} = p_k^{\text{pax}} \sum_{r \in \mathcal{R}_k} q_{rt}(\lambda_{rt}, \lambda_{-rt})$$

where ridership q_{rt} depends on the effective arrival rate of route r and the effective arrival rates of other routes λ_{-rt} , capturing demand spillovers within and across route bundles. The per-passenger price p_k^{pax} is set by the transit agency.

The service-based component captures revenue for kilometers of service supplied:

$$R_{kt}^{\text{dist}} = p_k^{\text{dist}} \sum_{r \in \mathcal{R}_k} f_{rdkt} L_r^s$$

where L_r^s is the route service distance. The per-kilometer price p_k^{dist} is determined in the competitive tender and fixed in the contract. Unlike passenger revenue, this component is purely mechanical: it scales linearly with service kilometers.

This dual revenue structure creates incentives for both ridership maximization and service provision.

Penalties and Quality Targets The transit agency establishes quality targets for frequency \bar{f}_r and service regularity \bar{CV}_r , for each route, with penalties for deviations:

$$\begin{aligned}\mathcal{P}^f(f_r, \bar{f}_r) &= \max\{0; \tau^f \cdot (\bar{f}_r - f_r)\} \\ \mathcal{P}^{\text{wait}}(f_r, \bar{f}_r, CV_r, \bar{CV}_r) &= \max\{0; \tau^w \cdot (W_r - \bar{W}_r)\}\end{aligned}$$

where W_r is the realized average wait time and \bar{W}_r is the target wait time. The relationship between service attribute choices and wait time follows the engineering formula:

$$W_r = \frac{1}{2f_r} \cdot (1 + CV_r^2)$$

This specification captures how both frequency and headway regularity affect passenger wait times, providing the link between supply-side operational decisions and demand-side service quality. While \mathcal{P}^f penalizes undersupply of frequency directly, $\mathcal{P}^{\text{wait}}$ internalizes the combined effect of frequency and regularity on waiting times.

Operational Costs Transit operations are labor intensive, so the cost structure should link labor inputs to the service attributes chosen by firms. The starting point is the vehicle-hour requirement implied by a given frequency and route characteristics:

$$\text{Vehicle-hours}_{rdkt} = f_{rdkt} \cdot \frac{L_r^T}{s_{rt}},$$

where L_r^T denotes the route distance including deadhead travel from the depot to the route origin, and s_{rt} is the average route speed. This measure differs from the service distance L_r^s that generates distance-based revenue, emphasizing the role of depot location in shaping costs.

Labor demand depends on both the scale and the quality of service provision. While vehicle-hours capture the quantity dimension, regularity requires additional managerial inputs such as dispatching and monitoring. I represent the production technology for

composite labor requirements as:

$$\text{Labor}_{rdkt} = \left(f_{rdkt} \cdot \frac{L_r^T}{s_{rt}} \right)^\gamma \cdot g(CV_{rdkt}),$$

where γ is an elasticity mapping vehicle-hours into labor units, and $g(CV_{rdkt})$ captures the incremental labor effort required to improve headway regularity. I assume $g(CV_{rdkt}) = CV_{rdkt}^{-\phi}$ with $\phi > 0$, so that reducing the coefficient of variation of headways entails increasing marginal labor requirements.

Route-level costs follow directly from multiplying labor demand by the input price. In addition, I allow for depot-level scale effects. Routes sharing a depot benefit from common resources such as maintenance facilities, supervisory staff, and spare vehicles. Rather than modeling depot aggregation explicitly, I incorporate these effects directly into the route-level specification. Combining the three dimensions quantity, quality, and scale effects yields:

$$C_{rdkt} = w_k \cdot \left(f_{rdkt} \cdot \frac{L_r^T}{s_{rt}} \right)^\gamma \cdot CV_{rdkt}^{-\phi} \cdot |\mathcal{R}_{dkt}|^\rho \cdot \varepsilon_{rdkt}, \quad (23)$$

where w_k is the firm-specific wage rate, $|\mathcal{R}_{dkt}|$ is the number of routes operated from depot d , and ε_{rdkt} captures route-level productivity shocks. A negative ρ reflects economies of scale, while a positive ρ reflects congestion effects. This expression captures the three key dimensions of operational costs: service quantity, service quality, and scale effects.

Optimality Conditions Transit operators maximize operational profit Π_k^{op} firms by choosing frequency f_{rdkt} and regularity measured by the coefficient of variation of headways CV_{rdkt} .

The first-order conditions for optimal frequency and regularity are:

$$\frac{\partial C_k}{\partial f_r} = p_k^{\text{pax}} \left[\frac{\partial q_r}{\partial \lambda_r} \frac{\partial \lambda_r}{\partial f_r} + \sum_{u \neq r} \frac{\partial q_u}{\partial \lambda_u} \frac{\partial \lambda_u}{\partial f_r} \right] + p_k^{\text{dist}} L_r^s - \frac{\partial \mathcal{P}^f}{\partial f_r} - \frac{\partial \mathcal{P}^{\text{wait}}}{\partial f_r} \quad (24)$$

$$\frac{\partial C_k}{\partial CV_r} = p_k^{\text{pax}} \left[\frac{\partial q_r}{\partial \lambda_r} \frac{\partial \lambda_r}{\partial CV_r} + \sum_{u \neq r} \frac{\partial q_u}{\partial \lambda_u} \frac{\partial \lambda_u}{\partial CV_r} \right] - \frac{\partial \mathcal{P}^{\text{wait}}}{\partial CV_r} \quad (25)$$

where $C_k = \sum_{r \in \mathcal{R}_k} C_{rdkt}$.

These conditions show that optimal service attribute decisions balance marginal costs against four sources of marginal benefit: direct ridership effects on the route, demand spillovers to other routes in the bundle, distance-based revenue, and the avoidance of regulatory penalties. The presence of demand spillovers $\sum_{u \neq r} \frac{\partial q_u}{\partial \lambda_u} \frac{\partial \lambda_u}{\partial f_r}$ illustrates that firms

internalize cross-route demand interactions within their bundle, a key mechanism for evaluating the welfare effects of bundling.

6.3 Road Technology

I model the road network as a directed graph, similar to Almagro *et al.* (2022), where each node represents a bus stop l , and edges connect contiguous bus stops. I assume that car routes are exogenous and travelers take the route suggested by Google Maps. The transit network is fixed but travelers choose which route or combination of routes to take endogenously, as explained in Section 6.1.2. A traveler going from bus stop l to bus stop l' follows a directed path over edges that connects l and l' .

During period n , the total vehicle flow on edge e is:

$$V_{en} = \sum_j \omega_j V_{enj}, \quad (26)$$

where V_{enj} is the total number of vehicles of mode j going through e and weights ω_j capture the fact that cars and buses may have different effects on congestion. For cars, the number of vehicles is a function of trips $V_{enj} = \sum_{m \in \mathcal{M}_{nj}^e} q_{mj}$, where \mathcal{M}_{nj}^e is the set of all markets in which travelers take a route that goes through edge e . For buses, the number of vehicles is a function of frequencies $V_{enj} = \sum_{r \in \mathcal{R}_{nj}^e} f_{rj}$, where \mathcal{R}_{nj}^e is the set of bus routes that go through e .

For road-based modes, the travel time over edge e at period n for mode j is given by:

$$T_{enj}^{\text{veh}} = \max\{T_{ej}^0, A_{enj} \cdot V_{enj}^\beta\}. \quad (27)$$

For every pair of neighboring bus stops, there is a range with low vehicle flows for which the travel time is independent of vehicle flows. Travel time is then equal to an edge-mode specific *free-flow time* T_{ej}^0 that captures road infrastructure and geography (including distance). The second term inside the maximum represents the range in which travel times increase with vehicle flows. Over that range, I assume a constant elasticity β of travel times to vehicle flows. A_{enj} is an edge-mode specific scale factor that captures geography and road infrastructure.

7 Estimation

7.1 Travel Preference Parameters

I estimate the set of travel preference parameters $\Omega = \{\theta_{ij}, \alpha_{\text{price}}, \alpha_{\text{veh}}, \alpha_{\text{wait}}, \mu_{\text{transfer}}\}$ for mode and route choice via maximum likelihood estimation (MLE).

Identification The identifying variation comes from the rich variation in choice alternative characteristics and observed choices made by travelers. The cost, in-vehicle travel time, wait time, and transfer penalty parameters are informed by how differences in these attributes across choice alternatives affect the relative odds of choosing different modes and routes.⁴ With choice sets ranging from 1 to 32 transit route options (median of 8), there is substantial cross-sectional variation in the attractiveness of transit relative to car travel and in the composition of available route alternatives.

I include an extensive set of fixed effects and control variables to address potential sources of bias in preference parameter estimation. The specification includes mode-specific fixed effects, mode-trip characteristic interactions (including trip distance, purpose, time period, and CBD origin/destination indicators), and mode-demographic interactions with traveler characteristics including education, age, and gender. These interactions control for a rich set of time-varying and location-specific unobservables by travel mode.

Parameter Estimates Table 2 reports the travel preference parameter estimates under four specifications. Columns (1)–(3) progressively add interactions of mode dummies with trip-related and demographic characteristics, while column (4) allows for random coefficients on mode dummies. Across all specifications, the coefficients are stable in magnitude and highly significant, which suggests that the estimates are not driven by specification choice.

The estimates indicate that commuters place a substantially higher disutility on waiting relative to in-vehicle travel time. In column (4), the marginal utility of one hour of waiting time is about 8.4, compared to 4.7 for an hour of travel time. This implies that waiting is valued at roughly 1.8 times in-vehicle travel, a ratio consistent with the literature and reinforcing the role of service frequency in determining demand. The implied willingness to pay for an additional bus per hour, shown in Figure 4a, highlights the steep marginal value passengers place on frequency improvements.

Cost sensitivity is also precisely estimated, with a marginal utility of -0.42 per dollar. Combining the time and cost coefficients yields an average value of travel time (VOT) between \$10.9–\$11.4 per hour across specifications, in line with benchmarks for urban commuting contexts. The transfer penalty is around -0.98 in utility units, which translates into a time-equivalent disutility of about 12–13 minutes of in-vehicle time. This penalty reflects the inconvenience of making a connection above and beyond the mechanical time costs of transferring.

Column (4) introduces heterogeneity in preferences for modes, with significant random

⁴The fare structure P_h varies across options within markets. While bus-to-bus transfers incur no additional cost, bus-to-subway transfers require an additional reduced fare, generating price variation that helps identify travel cost sensitivity.

coefficient estimates for both car and transit dummies.⁵ The standard deviations are sizeable (0.63 for car, 0.85 for transit), indicating meaningful dispersion in mode-specific tastes beyond observed demographics or trip features. This heterogeneity is important when simulating counterfactuals, as it governs substitution patterns in mode and route choices.

Taken together, these estimates underscore two main findings. First, wait time carries a disproportionate weight in commuter utility, which strengthens the rationale for policies that target service attributes such as frequency or regularity. Second, transfer penalties are sizeable but not dominant, suggesting that improving network connectivity may generate meaningful but more modest gains relative to frequency improvements.

7.2 Cost Parameters

I estimate the set of cost parameters $\Psi = \{\gamma, \phi, \rho\}$ for service attribute choices via generalized method of moments (GMM).

Identification Estimating the parameters of the route-level cost function in equation (23) is challenging because the variables of interest are chosen by firms, raising concerns about endogeneity. I address this using two complementary sources of exogenous variation. First, the contract reform introduced stricter quality targets for some routes and rebundled these routes across depots. I exploit this variation to identify the parameters linked to regularity and depot load. Second, for frequency and route speed, I rely on exogenous shocks or features of the network design. Below, I discuss the potential sources of bias for each variable and the instruments or assumptions I use to address them.

Frequency is chosen by operators and may respond to unobserved demand shocks. I instrument frequency with exogenous operational shocks—such as vehicle breakdowns, blockages, and other unexpected incidents—that constrain the number of buses that can be dispatched but are not systematically related to passenger demand.

Headway regularity may be correlated with unobserved productivity or demand conditions, for example if firms exert greater effort on high-demand routes. To address this concern, I exploit stricter quality targets introduced only for routes under new contracts, while old contract routes retained previous standards. This regulatory variation shifts the cost of achieving regularity but does not directly affect passenger preferences, since contract terms are not observed by travelers.

⁵For the specification with random coefficients, since there is no closed form for choice probabilities when integrating out the random preference distribution, I simulate the choice probabilities using Monte Carlo integration with a sequence of 100 Halton draws. This simulation approach maintains computational tractability while allowing for unobserved preference heterogeneity that is essential for welfare analysis.

Depot load can be endogenous if more routes are allocated to more efficient depots or to high-demand areas. To address this, I use depot reallocations from the reform's rebundling process, focusing on old contract routes that experienced depot changes but unchanged quality standards. These administrative reallocations altered depot load orthogonally to route-specific demand or productivity conditions.

Route speed is an equilibrium outcome: positive demand shocks may increase congestion and lower speeds. I instrument route speed with free-flow speeds during off-peak hours, which primarily reflect permanent infrastructure characteristics (e.g., road capacity, design) rather than contemporaneous demand shocks.

Route distance is determined by network design and depot location and is fixed over the estimation window, so I treat it as exogenous.

Parameter Estimates Table 3 reports the cost parameter estimates. The base labor elasticity parameter γ is estimated at 0.643, indicating that labor requirements scale less than proportionally with vehicle-hours. This relationship suggests the presence of fixed labor components in transit operations, such as supervisory staff or administrative overhead that do not increase one-for-one with service frequency. The magnitude implies that a 10% increase in vehicle-hours translates to approximately a 6.4% increase in labor requirements.

The quality parameter ϕ is estimated at -1.137, reflecting the additional labor costs associated with improving headway regularity. Since regularity enters the cost function as CV_{rdkt}^ϕ , this negative estimate indicates that reducing the coefficient of variation of headways (improving service quality) requires substantial additional labor inputs. The magnitude suggests that transit operators face steep marginal costs when attempting to provide more regular service, consistent with the intensive monitoring and dispatching efforts required to maintain schedule adherence.

The depot scale parameter ρ is estimated at -0.216, confirming the presence of economies of scale at the depot level. This negative coefficient indicates that routes sharing a common depot benefit from shared resources such as maintenance facilities, supervisory staff, and spare vehicles. The magnitude implies that a 10% increase in the number of routes operated from a depot reduces per-route costs by approximately 2.2%, demonstrating meaningful but modest scale economies in transit operations.

7.3 Road Technology Parameters

I estimate the congestion elasticity β by assuming that $a_{enj} = \log A_{enj} = \alpha_j + \varepsilon_{enj}$. Under this assumption, the estimating equation becomes:

$$\log T_{enj}^{\text{veh}} = \alpha_j + \beta \log V_{en} + \varepsilon_{enj}, \quad (28)$$

where α_j is a mode fixed effect that captures systematic level differences between car and bus travel times. The remaining error ε_{enj} captures unobservable shocks that vary across periods of the day within edge e .

Parameter Estimates Table 4 presents the road technology parameter estimates. I find elasticities of travel time with respect to traffic flows between 0.12 to 0.13, which are comparable with existing estimates in the literature (Akbar *et al.*, 2023). I also find that buses systematically move at about 70% of car speed along the same edges, regardless of congestion.

8 Counterfactuals

In each case, I compare market outcomes to the social planner's benchmark and report results as ratios relative to the planner's allocation. Ratios close to one indicate outcomes approaching the socially optimal allocation.

No Regulation The first counterfactual considers a setting without government intervention, in which firms and travelers interact directly in the transit market. Transit operators simultaneously choose fares and service attributes, while travelers choose modes and, conditional on selecting transit, routes. Figure 5 presents the results. Consumer surplus initially rises with firm entry, as competition reduces market power and drives down fares. However, beyond the entry of the fifth firm, consumer surplus declines due to service quality losses from uncoordinated operations. This reflects network fragmentation: additional operators introduce inefficiencies in service regularity and frequency choices, offsetting the gains from lower fares. Environmental externalities increase monotonically with entry, as weaker transit service induces more travelers to shift toward private car use. Producer surplus declines gradually with entry, but firms maintain significant local market power, so fares remain above the socially optimal level and do not decrease as rapidly as under perfect competition.

Optimal Quality Targets The second counterfactual introduces government intervention through optimally designed quality targets. These targets specify penalties that align

firms' incentives with the externalities internalized by the social planner. Figure 6 shows the resulting allocations. The introduction of optimal quality targets curtails service underprovision and reduces the inefficiencies associated with fragmented operations. In contrast to the no-regulation scenario, consumer surplus remains stable after the entry of the fifth firm, as quality standards mitigate the deterioration of service. Environmental externalities are also substantially reduced: the target design brings outcomes close to the socially optimal level. However, quality regulation does not address the pricing distortion, and firms continue to exert market power. As a result, fares remain above the planner's benchmark, and additional entry has only limited effects on price competition.

References

- AKBAR, P., COUTURE, V., DURANTON, G. and STOREYGARD, A. (2023). Mobility and congestion in urban India. *American Economic Review*, **113** (4), 1083–1111.
- ALMAGRO, M., BARBIERI, F., CASTILLO, J. C., HICKOK, N. and SALZ, T. (2022). *Optimal Urban Transportation Policy: Evidence from Chicago*. Working paper.
- BARWICK, P. J., KWON, H.-S. and LI, S. (2024). *Attribute-based Subsidies and Market Power: an Application to Electric Vehicles*. Working Paper 32264, National Bureau of Economic Research.
- , LI, S., WAXMAN, A. R., WU, J. and XIA, T. (2021). *Efficiency and Equity Impacts of Urban Transportation Policies with Equilibrium Sorting*. Working Paper 29012, National Bureau of Economic Research.
- BORDEU, O. (2023). *Commuting infrastructure in fragmented cities*. Working paper.
- BOSIO, E., DJANKOV, S., GLAESER, E. and SHLEIFER, A. (2022). Public procurement in law and practice. *American Economic Review*, **112** (4), 1091–1117.
- BRANCACCIO, G., KALOUPTSIDI, M. and PAPAGEORGIOU, T. (2020). Geography, transportation, and endogenous trade costs. *Econometrica*, **88** (2), 657–691.
- BUCHHOLZ, N. (2022). Spatial equilibrium, search frictions, and dynamic efficiency in the taxi industry. *The Review of Economic Studies*, **89** (2), 556–591.
- CHEN, Y. (2024). *Network Structure and the Efficiency Gains from Mergers: Evidence from US Freight Railroads*. Working paper.
- CONWELL, L. (2023). *Subways or Minibuses? Privatized provision of public transit*. Working paper.
- DEGIOVANNI, P. and YANG, R. Y. (2023). *Economies of scale and scope in railroading*. Working paper.
- FRECHETTE, G. R., LIZZERI, A. and SALZ, T. (2019). Frictions in a competitive, regulated market: Evidence from taxis. *American Economic Review*, **109** (8), 2954–2992.
- KREINDLER, G., GADUH, A., GRAFF, T., HANNA, R. and OLKEN, B. A. (2023). *Optimal Public Transportation Networks: Evidence from the World's Largest Bus Rapid Transit System in Jakarta*. Working Paper 31369, National Bureau of Economic Research.
- MBONU, O. and EAGLIN, F. C. (2024). *Market Segmentation and Coordination Costs: Evidence from Johannesburg's Minibus Networks*. Working paper.
- MUNIZAGA, M. A. and PALMA, C. (2012). Estimation of a disaggregate multimodal public transport origin-destination matrix from passive smartcard data from santiago, chile. *Transportation Research Part C: Emerging Technologies*, **24**, 9–18.
- WANG, B. (2024). Public transit provision and fare structure in U.S. cities. *Working Paper*.
- YUAN, Z. and BARWICK, P. J. (2024). *Network Competition in the Airline Industry: An Empirical Framework*. Working Paper 32893, National Bureau of Economic Research.

Tables and Figures

Table 1: Effect of Network Fragmentation on Service Quality

	Log Frequency (1)	Log CV of Headways (2)	Log Wait Time (3)
Log Concentration (HHI)	-0.138*** (0.006)	-0.224*** (0.007)	-0.027*** (0.003)
Covariates	X	X	X
Trip FEs	X	X	X
Date FEs	X	X	X
Origin FEs	X	X	X
Destination FEs	X	X	X
Observations	8,061,997	8,061,997	8,061,997
Within R ²	0.854	0.660	0.406

Notes: This table reports regression estimates of the relationship between network concentration and service quality. The unit of observation is a trip–origin–destination choice set on a given date, constructed from the household travel survey for the period August to December 2022. The dependent variables are the log of aggregate frequency, the log of the coefficient of variation of headways, and the log of expected wait time. The variable of interest is the log of the Herfindahl–Hirschman Index (HHI), constructed from route-level market shares based on planned frequencies. All regressions control for the total planned frequency and the number of routes in the market. Trip, date, origin, and destination fixed effects are included, and standard errors are clustered at the traveler level. *** $p < 0.01$, ** $p < 0.05$, * $p < 0.1$.

Table 2: Travel Preference Parameters

	(1)	(2)	(3)	(4)
Wait time (hr)	-8.077*** (0.139)	-8.394*** (0.148)	-8.368*** (0.149)	-8.356*** (0.148)
Travel time (hr)	-4.585*** (0.080)	-4.620*** (0.082)	-4.763*** (0.084)	-4.655*** (0.080)
Cost (\$)	-0.410*** (0.015)	-0.412*** (0.015)	-0.416*** (0.016)	-0.424*** (0.015)
Transfer penalty	-0.954*** (0.022)	-0.985*** (0.023)	-0.988*** (0.023)	-0.979*** (0.026)
Random coefficients on mode dummies (σ_j)				
Car				0.628*** (0.068)
Transit				0.848*** (0.090)
Mode FE	Yes	Yes	Yes	Yes
Mode \times Trip Related FE	No	Yes	Yes	Yes
Mode \times Demographics FE	No	No	Yes	Yes
Log-likelihood	-50932.6	-50814.0	-48557.7	-48331.6
Mean VOT (\$/hr)	11.2	11.2	11.4	10.9
Observations	49,157	49,157	49,157	49,157

Notes: This table reports travel preference parameter estimation results from the specifications outlined in section 7.1. The estimation sample is based on the full set of trips. The parameters are estimated via MLE. VOT stands for value of time measure in dollar per hour. Mode-Trip related fixed effects include trip distance, purpose, time period, and CBD origin/destination indicators. Mode-Demographics fixed effects include education, age, and gender. Standard errors in parentheses. *** p < 0.01, ** p < 0.05, * p < 0.1.

Table 3: Cost Parameters

	(1)
Base Labor (γ)	0.643*** (0.058)
Quality (ϕ)	1.137*** (0.015)
Depot scale (ρ)	-0.216*** (0.052)
Observations	152,883

Notes: This table reports cost parameter estimation results. The parameters are estimated via GMM. *** p < 0.01, ** p < 0.05, * p < 0.1.

Table 4: Road Technology Parameters

	Log Travel Time		
	(1)	(2)	(3)
Car Constant	-0.361*** (0.077)	-0.400*** (0.084)	-0.400*** (0.084)
Log Traffic Flow	0.130* (0.061)	0.124*** (0.037)	0.119** (0.036)
Monitoring Station FEs		X	X
Date FEs			X
Observations	70,174	70,174	70,174
Within R ²	0.128	0.128	0.128

Notes: This table reports regression estimates of the relationship between traffic flow and travel times. The unit of observation is a traffic monitoring station, measured in 15-minute intervals between 6am and 9pm. The dependent variable is the log of travel time (in hours) for the corresponding road segment. The independent variable is the log of vehicle flows, measured in vehicles per hour. The regression is pooled across cars and buses, with a mode-specific constant capturing systematic differences in travel times between modes. The sample covers 64 traffic monitoring stations across 9 municipalities and is restricted to cases where flow per lane is below 1,100 vehicles per hour. This threshold corresponds to the maximum capacity of a lane in urban areas with intersections and traffic lights and retains 99.4% of the observations. Standard errors are clustered at the municipality level. *** p < 0.01, ** p < 0.05, * p < 0.1.

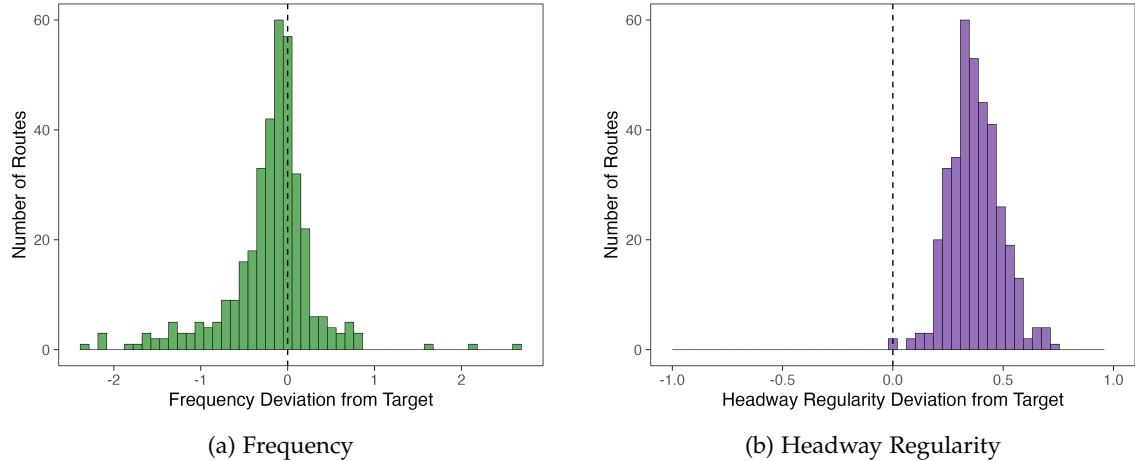


Figure 1: Distribution of Deviations from Planned Transit Service Attributes (Pre-Reform Period).

Notes: Panel (a) shows the distribution of average frequency deviations (observed minus planned frequency) across transit routes during the pre-reform period. Panel (b) displays the distribution of coefficient of variation deviations for headway regularity (observed minus planned variability). The vertical dashed line at zero represents perfect adherence to planned schedules. Colors distinguish routes operated by different firms.

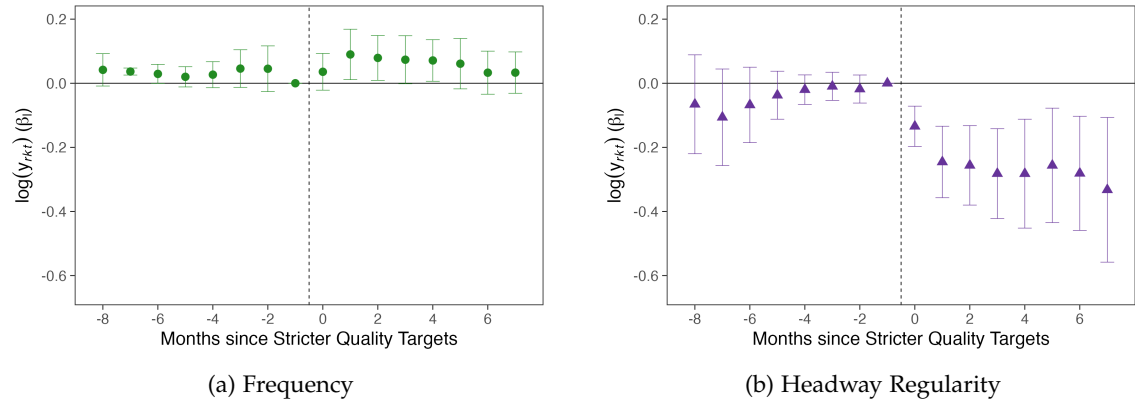


Figure 2: Effect of Stricter Quality Targets on Transit Service Attributes.

Notes: The figures show event study estimates of the impact of stricter quality targets on transit service outcomes, with time measured in months relative to policy implementation. Panel (a) displays the effects on service frequency, showing relatively stable coefficients in the pre-treatment period followed by a slight increase in frequency levels after the policy implementation. Panel (b) shows the effects on headway regularity (measured in coefficient of variation), with pre-treatment estimates fluctuating around zero and post-treatment effects indicating improved headway regularity (negative coefficients suggest lower variability in headways). Error bars represent 95% confidence intervals, and estimates control for firm, route, and time fixed effects.

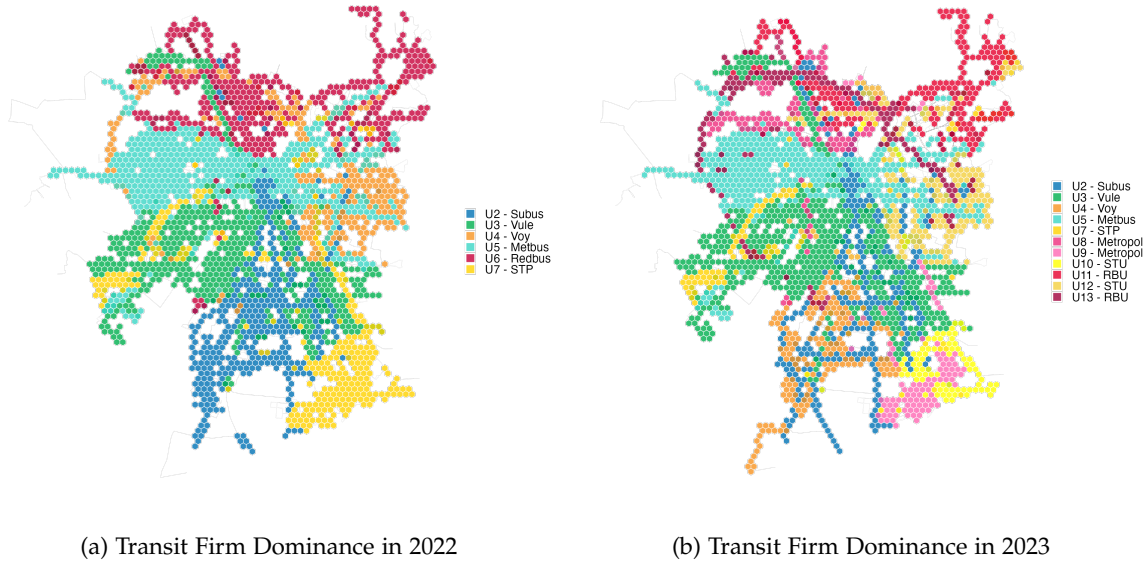


Figure 3: Network Fragmentation Before and After the Reform.

Notes: The figures display transit network fragmentation through geographic dominance of transit firms using a hexagonal grid overlay. Panel (a) shows the transit network in 2022 before the rebundling and tendering process, while Panel (b) shows the transit network in 2023. Each hexagon represents a spatial area where a single transit firm operates the plurality of routes and holds more than 25% of the local route share, with a minimum threshold of 3 routes per hexagon. Colors correspond to different transit operators as shown in the legend. Areas without hexagons indicate either insufficient route density or high fragmentation where no single firm achieves dominance.

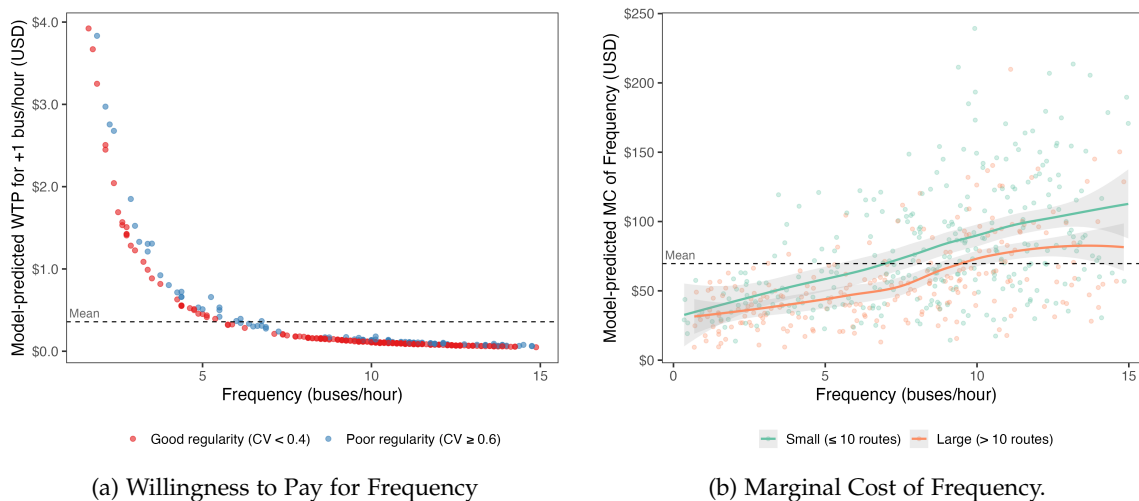


Figure 4: Frequency - Demand and Supply

Notes: The figures show .

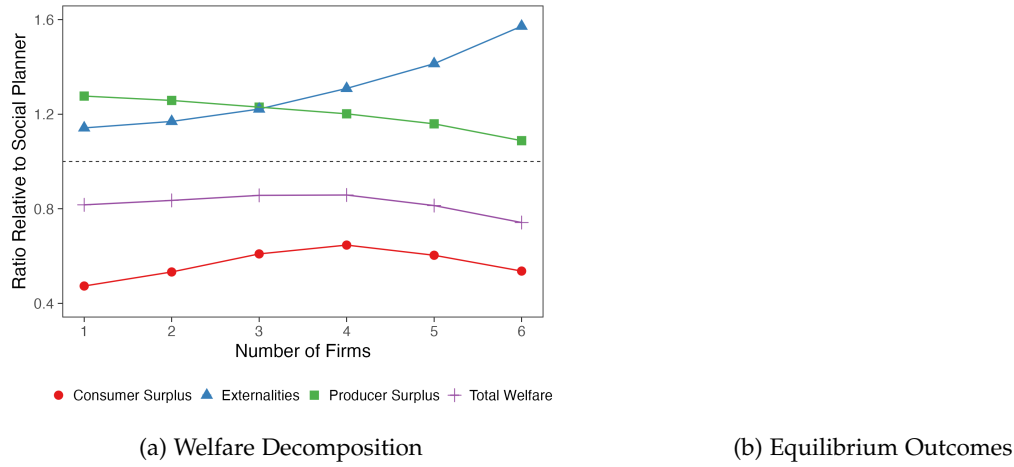


Figure 5: Counterfactual Scenario: No Regulation

Notes: The figures show .

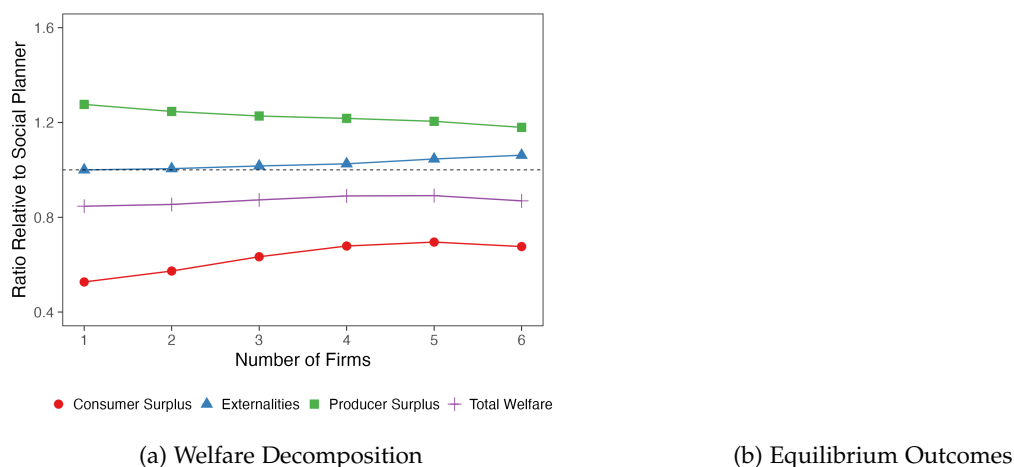


Figure 6: Counterfactual Scenario: Optimal Quality Targets

Notes: The figures show .

Appendix A Data sources

Santiago Household Travel Survey (SHTS) Data

The sample size was determined using the Smith method to establish the number of surveys required in each of the municipality, ensuring estimation of trip generation rates, modal shares, and car ownership rates. Within each municipality, blocks were selected through probability proportional to size (PPS) sampling with replacement. A minimum of 160 surveys were conducted in each municipality—100 on weekdays and 60 on weekends.

The total sample includes 18,264 households, with 11,246 surveyed on weekdays during the normal season and 7,018 surveyed on weekends, covering both normal and summer seasons. Surveys conducted during the normal season took place between July 2012 and November 2013, while summer season surveys were carried out in January and February 2013.

Data collection was conducted in person using mobile devices and involved two visits. During the first visit, surveyors introduced the study, gathered household-level information, and assigned a random travel day for each household member. Participants received a travel diary to record their trips on the assigned day. The second visit involved collecting trip data through in-person interviews with each household member. If any household member was unavailable, the surveyor returned until all trip data were collected. This methodology substantially reduces the underreport issue of surveys based on collecting the trips taken during the preceding 24 hours.

The SHTS includes detailed individual (e.g., age, gender, number of trips, driver license, education level, occupation, and income) and household demographics (e.g., georeferenced location, household size, number of vehicles, rent or mortgage, household income) and trip characteristics (georeferenced origin and destination, purpose, mode choice, travel time, period of day).

I restrict my sample to the municipalities within the urban area of Santiago which involves 13,696 households, 31,735 travelers and 74,166 trips.

I drop the observations that take a mode of transportation different than car, public transit, or walking (15.73%) I drop the observations with purpose other than work, study or other (0.38%). I drop the observations with implausible trip distance and travel time (0.43%). I drop the observations with missing income (0.44%). I drop observations with incomplete cases (0.01%). After doing this, my final trip dataset contains 12,668 households, 27,111 travelers, and 61,574 trips.

The monetary cost for walking is zero. The public transit fare is flat for buses over the day at 1.1 USD and varies by period (peak and off-peak) for subway –1.3 or 1.2 USD–. Transfers are free within a period of 1.5 hours except for transfers between bus and subway, in which the traveler pays a small fee to cover the subway fare. High school students don't pay and college students have a flat fare of 0.4 USD. Fuel cost is a major component of the monetary cost associated with driving. Based on the average fuel economy reported by XXX, I use 0.11 liter/km (9 km/liter). Gasoline prices are XXX USD/liter.

Appendix B Model estimation

Appendix C Figures and tables (for online publication)

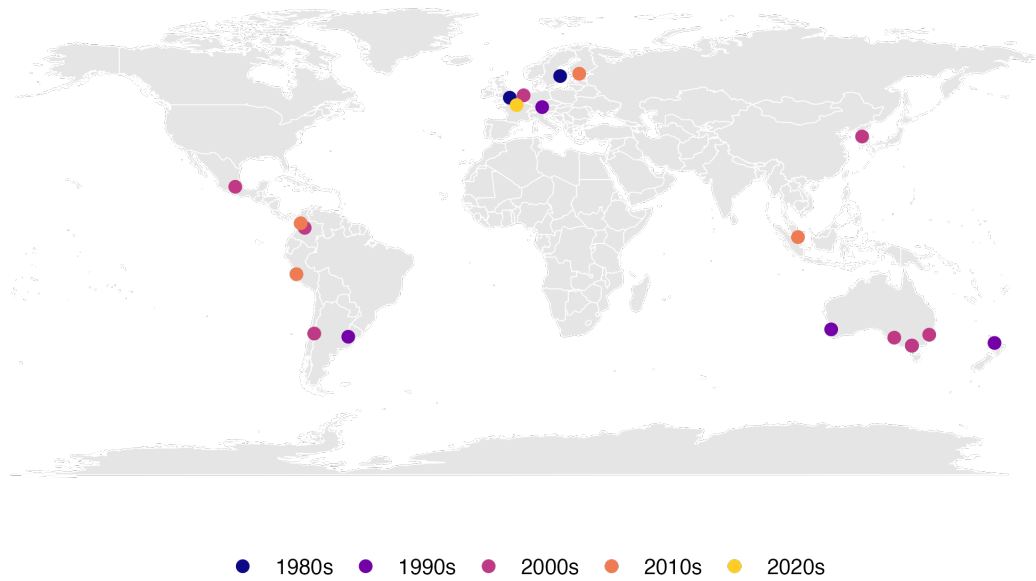


Figure C.1: Geographic distribution of cities adopting competitive tendering for public transit, by decade.

Table C.1: Mode Choice Summary Statistics

	N	Mean	SD
Panel A: Household Characteristics			
Household size	11,612	3.40	1.56
Vehicle ownership	11,612	0.47	0.50
Household number of vehicles	11,612	0.58	0.73
Income: < USD 10k	11,612	0.31	0.46
Income: [USD 10k, 40k)	11,612	0.60	0.49
Income: > USD 40k	11,612	0.09	0.28
Panel B: Traveler Characteristics			
Age (in years)	22,653	38.39	20.39
Female (= 1)	22,653	0.52	0.50
Education: Less than High School	22,653	0.24	0.42
Education: High School	22,653	0.43	0.49
Education: Associate degree	22,653	0.09	0.29
Education: College degree or higher	22,653	0.25	0.43
Panel C: Trip Characteristics			
Car available (= 1)	47,622	0.44	0.50
Origin within CBD (= 1)	47,622	0.31	0.46
Destination within CBD (= 1)	47,622	0.31	0.46
Driving (= 1)	47,622	0.39	0.49
Public Transit (= 1)	47,622	0.37	0.48
Walking (= 1)	47,622	0.25	0.43
Distance: [0 km, 2 km)	47,622	0.39	0.49
Distance: [2 km, 5 km)	47,622	0.23	0.42
Distance: > 5 km	47,622	0.38	0.48
Purpose: Work	47,622	0.32	0.47
Purpose: Study	47,622	0.15	0.36
Purpose: Other	47,622	0.53	0.50

Notes: This table presents summary statistics for transportation mode choice decisions. Sample includes all observations from the travel preference parameters estimation sample covering the period 2012-2013. All monetary values are in 2013 USD.

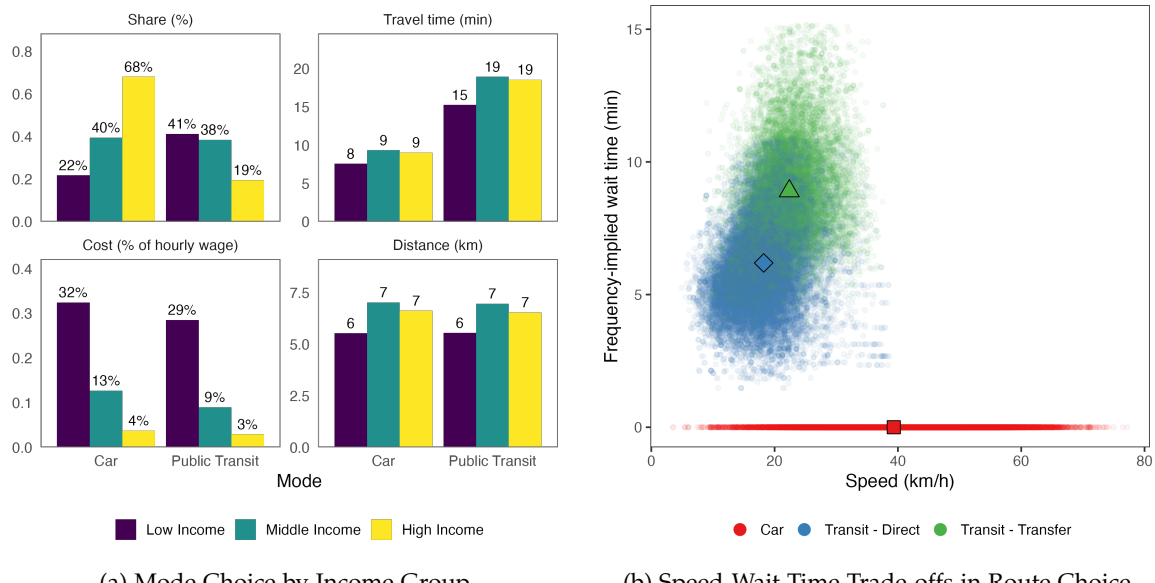


Figure C.2: Transportation Mode and Route Choice Patterns.

Notes: Panel (a) displays mode choice distributions across income groups, showing share, travel time, cost (as percentage of hourly wage), and distance for car versus public transit users. The displayed shares represent only car and public transit usage, with walking serving as the outside option to bring total mode shares to 100%. High-income travelers show greater car usage (68% vs 21.8% for low-income), while public transit users face longer travel times but lower relative costs. Panel (b) illustrates the speed-frequency trade-off in route choice, plotting frequency-implied wait times against travel speeds. The scatter plot reveals distinct clusters for different route types: cars, direct transit routes, and transfer-based transit options. Squared, Triangular and diamond markers indicate mean values for different route categories.

Table C.2: Route Choice Summary Statistics

	Direct		Transfer	
	Mean	SD	Mean	SD
Panel A: Off-peak				
Number of options	3.13	3.07	5.38	6.95
At least one option (= 1)	0.83	0.37	0.73	0.45
Subway (= 1)	0.11	0.31	0.43	0.49
Fare (USD)	1.10	0.30	1.11	0.31
Travel time (min)	12.97	11.05	19.72	13.21
Wait time (min)	3.93	1.01	7.57	1.46
Panel B: Peak				
Number of options	2.34	2.47	4.31	6.06
At least one option (= 1)	0.77	0.42	0.66	0.47
Subway (= 1)	0.12	0.32	0.46	0.50
Fare (USD)	1.09	0.33	1.15	0.34
Travel time (min)	16.08	13.07	27.06	14.56
Wait time (min)	3.61	1.10	7.01	1.61

Notes: This table presents summary statistics for route choice decisions. Sample includes all observations from travel preference parameters estimation sample covering the period 2012-2013. All monetary values are in 2013 USD.

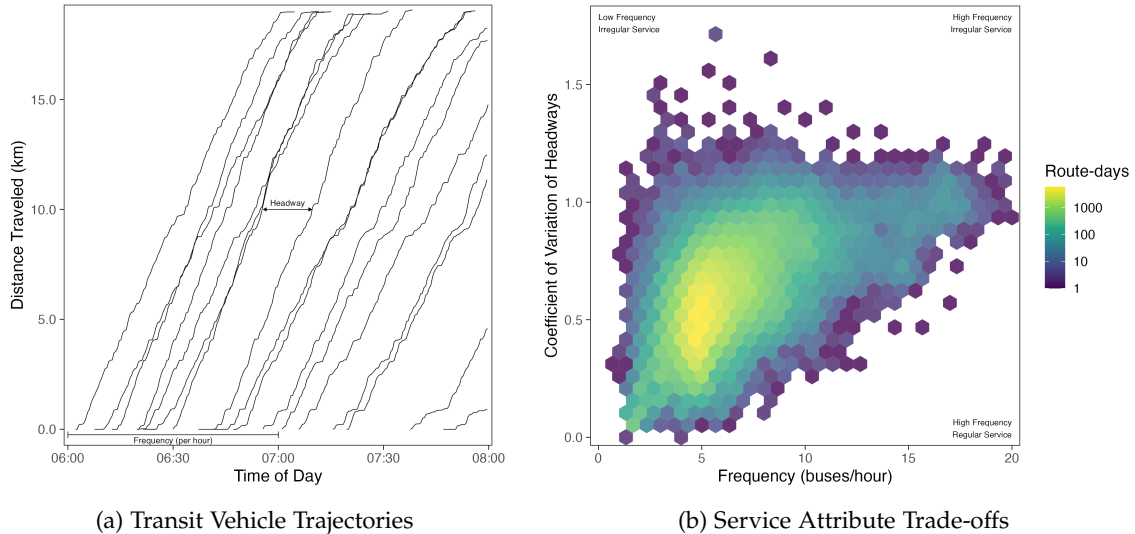


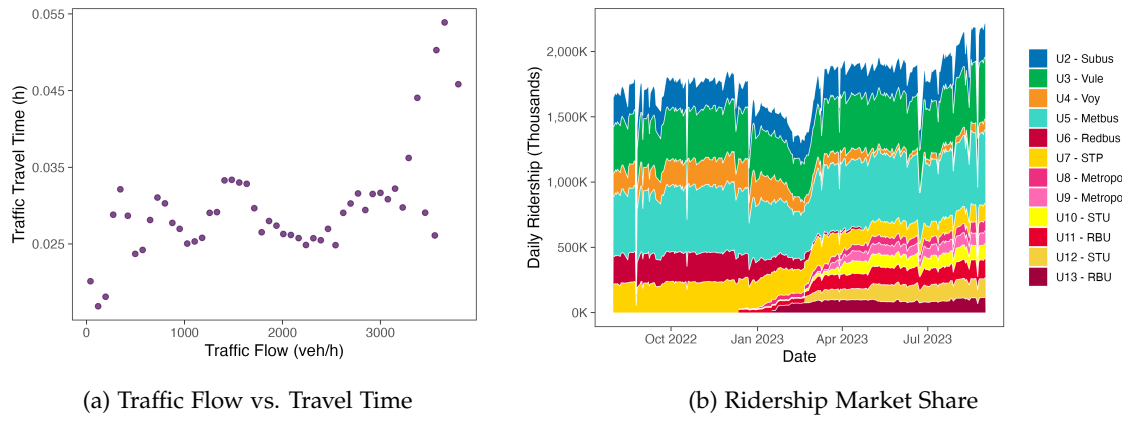
Figure C.3: Frequency and Headway Regularity Choice Patterns.

Notes: Panel (a) shows transit vehicle trajectories over time, illustrating frequency and headway concepts through dispatch timing and distance traveled. Panel (b) reveals the strategic trade-off between service frequency and observed reliability (coefficient of variation of headways), with density patterns showing common operational strategies.

Table C.3: Public Transit Supply Summary Statistics

	Mean	SD	Min	Max
Panel A: System-level				
Number of Bundles	8.50	2.53	6.00	11.00
Number of Firms	7.00	1.01	6.00	8.00
Number of Depots	65.84	2.05	62.00	68.00
Number of Routes	354.86	10.86	295.00	363.00
Daily Ridership (millions)	1.86	0.32	0.43	2.21
Panel B: Bundle-level				
Number of Depots	8.10	6.03	2.00	19.00
Number of Routes	41.75	23.67	11.00	89.00
Daily Ridership (thousands)	218.72	145.45	49.48	562.91
Panel C: Route-level				
Frequency (bus/h)	5.82	1.96	1.06	20.27
Headway Regularity (CV)	0.41	0.15	0.02	1.42
Length (km)	18.45	8.58	2.35	57.22
Speed (km/h)	17.83	3.32	1.44	39.29
Daily Ridership (hundreds)	28.52	24.72	0.01	170.64

Notes: This table presents summary statistics for public transit supply characteristics across three levels of aggregation. The sample includes route-day level observations from August 2022 and August 2023 to capture initial and final equilibrium states, excluding transient periods. Panel A shows system-level statistics aggregated across all bundles and routes. Panel B presents bundle-level statistics, where bundles represent groups of routes operated under the same contract. Panel C displays route-level characteristics including service frequency (buses per hour), headway regularity measured by coefficient of variation (CV), route length, average speed, and ridership.



(a) Traffic Flow vs. Travel Time

(b) Ridership Market Share

Figure C.4: Equilibrium Outcomes: Traffic Flow, Traffic Speed, and Ridership.

Notes: Panel (a) illustrates the traffic flow-travel time relationship. The gray points represent individual observations, while the purple line shows the binned averages. Panel (b) displays daily ridership trends across transit firms from August 2022 to August 2023, with each colored area representing a different operator's passenger volume. The stacked area chart shows bus system ridership fluctuating between approximately 1.6-2.2 million daily passengers.